

Electrochemical Genotoxicity Screening for Arylamines Bioactivated by *N*-Acetyltransferase

Minjeong So,[†] Eli G. Hvastkovs,[†] Besnik Bajrami,[†] John B. Schenkman,[‡] and James F. Rusling^{*†‡}

Department of Chemistry, 55 North Eagleville Road, University of Connecticut, Storrs, Connecticut 06269, and Department of Cell Biology, University of Connecticut Health Center, Farmington, Connecticut 06032

Genotoxicity screening sensors that measure DNA damage from metabolism of arylamines were developed and evaluated. The sensors feature ultrathin films containing DNA and *N*-acetyltransferase (NAT) on pyrolytic graphite (PG) electrodes. NAT in the film catalyzed the conversion of the arylamine 2-aminofluorene (2-AF) to 2-acetylaminofluorene (2-AAF) by acetyl coenzyme A (AcCoA) dependent *N*-acetylation, as verified by liquid chromatography. DNA damage in the films from exposure to reactive 2-AF metabolites was measured subsequent to the enzyme reaction using catalytic voltammetric oxidation with Ru(bpy)₃²⁺. Square wave voltammetric (SWV) peaks increased with enzyme reaction time, and relative DNA damage rates at pH 5.8 were measured within 2 min. Control incubations of DNA/NAT films without AcCoA gave no significant sensor response. CapLC–MS/MS analysis of 2-AAF/DNA reaction products was consistent with 2-AF-guanine adducts formed in the films. DNA damage occurred more rapidly under weakly acidic conditions (pH 5.5–5.8) than at neutral pH, suggesting that genotoxicity from arylamine metabolism by NAT could be more significant in slightly acidic environments.

Toxicity issues result in about 30% of drug development failures, so that reliable early toxicity screening may contribute to lower future costs.¹ Lipophilic molecules or their enzyme-generated metabolites can react with DNA in the human liver and often produce covalently bound nucleobase adducts.^{2–5} This process is called genotoxicity, and nucleobase adducts are biomarkers for reactive metabolites, xenobiotic exposure, and diseases such as cancer. Bioactivation of lipophilic pollutants or drugs by so-called phase I enzymes in the human liver, typified by cytochrome (cyt) P450s,^{6,7} is a major source of genotoxicity.

We previously described rapid, inexpensive biosensors and arrays for genotoxicity screening that detect cyt P450 enzyme-induced DNA damage.^{1,8–10} These biosensors feature thin films of DNA and metabolic enzymes immobilized on an electrode or in an array.^{11,12} Enzymes in the films metabolize a drug or pollutant molecule, creating possible reactive metabolites, which may form DNA adducts. DNA damage is detected by catalytic voltammetry using ruthenium bipyridyl (RuBPY) complexes¹³ or by electrochemiluminescence from a RuBPY–polyvinylpyridine polymer in the enzyme–DNA film.^{12,14,15} When ds-DNA is damaged by adduct formation, the signal in these sensors increases because the double helix is distorted improving accessibility of guanines to the catalyst and increasing the electrocatalytic reaction rate.^{9,16}

Alternative, but more complex and costly, genotoxicity screening can employ LC–MS/MS analysis of hydrolyzed DNA from DNA–enzyme films similar to those used in the sensors and provides identification and rates of formation of major nucleobase adducts.^{17,18} Response of sensors using phase I cyt P450 enzymes gave excellent correlations with nucleobase formation rates from LC–MS and with animal genotoxicity indices.¹⁸ High throughput sensor arrays based on the same principles have been used to provide information on the relative rates at which cyt P450 enzymes produce reactive metabolites.^{11,12}

To screen genotoxicity responses more realistically predictive of human in vivo response, enzymes in the sensors need to be expanded to enzymes beyond the phase I level. An eventual goal

* To whom correspondence should be addressed. E-mail: james.rusling@uconn.edu.

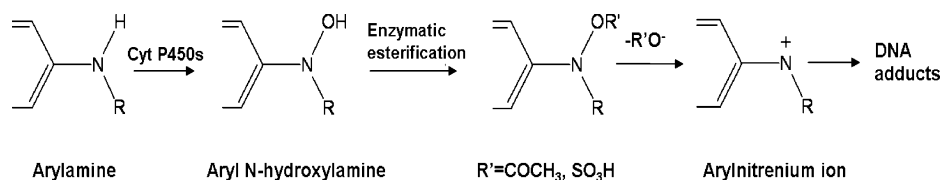
[†] Department of Chemistry, University of Connecticut.

[‡] Department of Cell Biology, University of Connecticut Health Center.

- (1) Rusling, J. F.; Hvastkovs, E. G.; Schenkman, J. B. *Curr. Opin. Drug Discovery Dev.* **2007**, *10*, 67–73 and references therein.
- (2) Singer, B.; Grunberger, D. *Molecular Biology of Mutagens and Carcinogens*; Plenum Press: New York, 1983.
- (3) Jacoby, W. B., Ed. *Enzymatic Basis of Detoxification*; Academic: New York, 1980; Vols I and II.
- (4) Friedberg, E. C. *Nature* **2003**, *421*, 436–440.
- (5) Scharer, O. D. *Angew. Chem., Int. Ed.* **2003**, *42*, 2946–2974.
- (6) Schenkman, J. B.; Greim, H., Eds. *Cytochrome P450*; Springer-Verlag: Berlin, Germany, 1993.

- (7) Ortiz de Montellano, Ed. *Cytochrome P450*; Kluwer/Plenum: New York, 2005.
- (8) Rusling, J. F. *Biosens. Bioelectron.* **2004**, *20*, 1022–1028.
- (9) Zhou, L.; Yang, J.; Estavillo, C.; Stuart, J. D.; Schenkman, J. B.; Rusling, J. F. *J. Am. Chem. Soc.* **2003**, *125*, 1431–1436.
- (10) Rusling, J. F.; Zhang Z. *In Biomolecular Films*; Rusling, J. F., Ed.; Marcel Dekker: New York, 2003; pp 1–64.
- (11) Wang, B.; Jansson, I.; Schenkman, J. B.; Rusling, J. F. *Anal. Chem.* **2005**, *77*, 1361–1367.
- (12) Hvastkovs, E. G.; So, M.; Krishnan, S.; Bajrami, B.; Tarun, M.; Jansson, I.; Schenkman, J. B.; Rusling, J. F. *Anal. Chem.* **2007**, *79*, 1897–1906.
- (13) (a) Johnston, D. H.; Glasgow, K. C.; Thorp, H. H. *J. Am. Chem. Soc.* **1995**, *117*, 8933–8938. (b) Weatherly, S. C.; Yang, I. V.; Thorp, H. H. *J. Am. Chem. Soc.* **2001**, *123*, 1236–1237.
- (14) Dennany, L.; Forster, R. J.; Rusling, J. F. *J. Am. Chem. Soc.* **2003**, *125*, 5213–5218.
- (15) So, M.; Hvastkovs, E. G.; Schenkman, J. B.; Rusling, J. F. *Biosens. Bioelectron.* **2007**, *23*, 492–498.
- (16) Zhou, L.; Rusling, J. F. *Anal. Chem.* **2001**, *73*, 4780–4786.
- (17) (a) Tarun, M.; Rusling, J. F. *Anal. Chem.* **2005**, *77*, 2056–2062. (b) Yang, J.; Wang, B.; Rusling, J. F. *Mol. Biosys.* **2005**, *1*, 251–259. (c) Tarun, M.; Bajrami, B.; Rusling, J. F. *Anal. Chem.* **2006**, *78*, 624–627.
- (18) Tarun, M.; Rusling, J. F. *Crit. Rev. Eukaryotic Gene Expression* **2005**, *15*, 295–315.

Scheme 1



Scheme 2



is to develop arrays containing a full complement of metabolic enzymes that could lead to genotoxicity. This paper describes the first step toward this goal, i.e., the incorporation of a phase II enzyme into a genotoxicity biosensor format.

Aromatic amines (AA) and heterocyclic aromatic amines (HAA) are potent mutagens whose metabolites form DNA adducts.¹⁹ A major pathway of AA/HAA bioactivation involves initial oxidation by hepatic cyt P450 enzymes to more reactive *N*-hydroxylamine derivatives.²⁰ This is followed by phase II metabolism by enzymes including *N*-acetyltransferase (NAT) and sulfotransferase to generate highly reactive *O*-substituted *N*-hydroxylamine intermediates²¹ (Scheme 1) that undergo spontaneous heterolysis of the N–O bond to generate arylnitrenium ions. These electrophilic reactive metabolites form adducts at the C8 position of guanines, affecting gene transcription and replication.²² In some cases, the hydroxylamine undergoes acid-catalyzed solvolysis generating reactive nitrenium ions that covalently modify DNA with similar consequences.^{23,24}

N-acetyltransferases (NATs, EC 2.3.1.5) occur in a wide range of organisms and vary in size from 30 to 34 kDa. They catalyze biotransformation of drugs and environmental xenobiotics that can have the aforementioned toxicological and carcinogenic consequences.^{25,26} As shown in Scheme 2, NATs catalyze the transfer of an acetyl group from acetyl coenzyme A (AcCoA) to a variety of aromatic amines, hydrazines, and hydrazides.

Enzymatic acetylation proceeds via a two-step ping-pong type mechanism. A conserved cysteine residue at the active site of NAT enzymes accepts the acetyl group of AcCoA to form an acetyl–enzyme intermediate in the first half reaction and then transfers it to the acceptor substrate in the second half reaction.^{26–28} The rate determining step in *N*-acetylation for mammalian NATs depends on the structure and basicity of the substrate. Certain human individuals have been categorized as slow acetylators or fast acetylators, raising the possibility of interindividual differences

in toxicity via this NAT metabolism.²⁹ The role of acetylation in the bioactivation of AA/HAA is species and substrate dependent. Specific examples include *N*-acetylation of arylamines or hydrazines, *O*-acetylation of *N*-hydroxylamines, and intramolecular acyl transfer with hydroxyarylacetamides. Most NAT enzymes also possess *O*-acetyltransferase activity.³⁰

Because of the difficulty in oxidizing acetylated aromatic amines,²⁴ *N*-acetylation becomes part of a detoxification process if the acetylated metabolite is excreted before bioactivation.³¹ However, some reports indicate that *N*-acetylation may result in reactive metabolites that further damage genetic and cellular material.^{32,33} Of the NAT isozymes, NAT1 acetylates substrates rapidly and NAT2 acetylates slowly. The rate of acetylation may be a key hereditary metabolic factor in determining individual susceptibility to arylamine-induced cancer.²⁹ Batracylin (8-aminoindolo[1,2-*b*]quinazolin-12(10*H*)-one; BAT) is a heterocyclic amine exhibiting antitumor activity. However, the kinetics of BAT *N*-acetylation in human liver showed that *N*-acetylation contributes to the toxicity of BAT and rapid acetylators would be at greater risk of developing adverse drug-induced effects than slow acetylators.^{34,35} Bioactivation of benzidine, an aromatic diamine, through *N*-acetylation has been shown to be a key step in the etiology of certain types of bladder cancers in humans.^{31,36}

In the present work, 2-aminofluorene (2-AF) was chosen as a test compound because of its well-known NAT-mediated metabolic pathway. NAT metabolizes 2-AF forming 2-acetyl aminofluorene (2-AAF) that can undergo further activation or detoxification reactions. 2-AF was synthesized as a potential pesticide but never approved by FDA due to the carcinogenicity of its amide derivative 2-AAF.³⁷ 2-AF and 2-AAF have been intensively studied and form primarily adducts at the C8 position of guanine in DNA.^{23,38–40}

Arylamine–DNA adducts are biomarkers for environmental arylamine exposure. 2-AF–DNA adduct formation in mice was

- (19) Turesky, R. J. *Drug Metab. Rev.* **2002**, *34*, 625–650.
 (20) Anari, M. R.; Josephy, P. D.; Henry, T.; O'Brien, P. J. *Chem. Res. Toxicol.* **1997**, *10*, 582–588.
 (21) Schut, H. A. J.; Snyderwine, E. G. *Carcinogenesis* **1999**, *20*, 353–368.
 (22) Lukin, M.; de los Santos, C. *Chem. Rev.* **2006**, *106*, 607–686.
 (23) Bonala, R. R.; Torres, M. C.; Attaluri, S.; Iden, C. R.; Johnson, F. *Chem. Res. Toxicol.* **2005**, *18*, 457–465.
 (24) Borosky, G. L. *Chem. Res. Toxicol.* **2007**, *20*, 171–180.
 (25) Hein, D. W.; McQueen, C. A.; Grant, D. M.; Goodfellow, G. H.; Kadlubar, F. F.; Weber, W. W. *Drug. Metab. Dispos.* **2000**, *28*, 1425–1432.
 (26) Wang, H.; Vath, G. M.; Gleason, K. J.; Hanna, P. E.; Wagner, C. R. *Biochemistry* **2004**, *43*, 8234–8246.
 (27) Mushtaq, A.; Payton, M.; Sim, E. J. *Biol. Chem.* **2002**, *277*, 12175–12181.
 (28) Rodrigues-Lima, F.; Delomenie, C.; Goodfellow, G. H.; Grant, D. M.; Dupret, J. M. *Biochem. J.* **2001**, *356*, 327–334.

- (29) Weber, W. W.; Hein, D. W. *Pharmacol. Rev.* **1985**, *37*, 25–79.
 (30) Summerscales, J. E.; Josephy, P. D. *Mol. Pharmacol.* **2004**, *65*, 220–226.
 (31) Zenser, T. V.; Lakshmi, V. M.; Rustan, T. D.; Doll, M. A.; Deitz, A. C.; Davis, B. B.; Hein, D. W. *Cancer Res.* **1996**, *56*, 3941–3947.
 (32) Kirilin, W. G.; Trinidad, A.; Yerokun, T.; Ogolla, F.; Ferguso, R. J.; Andrews, A. F.; Brady, P. K.; Hein, D. W. *Cancer Res.* **1989**, *49*, 2448–2454.
 (33) Chung, J. G.; Levy, G. N.; Weber, W. W. *Drug. Metab. Dispos.* **1993**, *21*, 1057–1063.
 (34) Stevens, G. J.; Payton, M.; Sim, E.; Mcqueen, C. A. *Drug. Metab. Dispos.* **1999**, *27*, 966–971.
 (35) Stevens, G. J.; Burkey, J. L.; Mcqueen, C. A. *Cell Biol. Toxicol.* **2000**, *16*, 31–39.
 (36) Martin, C. N.; Beland, F. A.; Roth, R. W.; Kadlubar, F. F. *Cancer Res.* **1982**, *42*, 2678–2696.
 (37) Heflich, R. H.; Neft, R. E. *Mutat. Res.* **1994**, *318*, 73–174.
 (38) Yasui, M.; Dong, H.; Bonala, R. R.; Suzuki, N.; Ohmori, H.; Hanaoka, F.; Johnson, F.; Grollman, A. P.; Shibutani, S. *Biochemistry* **2004**, *43*, 15005–15013.
 (39) Hoffmann, G. R.; Fuchs, R. P. P. *Chem. Res. Toxicol.* **1997**, *10*, 347–359.
 (40) Patel, D. J.; Mao, B.; Gu, Z.; Hingerty, B. E.; Gorin, A.; Basu, A. K.; Brody, S. *Chem. Res. Toxicol.* **1998**, *11*, 391–407.

used as an indicator of arylamine-induced DNA damage.⁴¹ NAT inhibitor studies in rat glial tumor cells,⁴² mouse leukemia cells,⁴³ and human bladder carcinoma cells⁴⁴ showed good correlation with 2-AF–DNA adduct formation. NAT-generated electrophiles leading to 2-AF–nucleobase adducts is thought to be a predominant pathway for mutagenic and carcinogenic effects associated with exposure to arylamines.⁴⁵ The metabolism of 2-AF is complex, and steps other than N-acetylation can influence bioactivation and nucleobase adduct formation, including N-hydroxylation, sulfonation, and deacetylation.^{41,46,47} Therefore, there is a need to ascertain the definitive enzymatic reaction(s) that imparts genotoxicity to the 2-AF substrate.

Herein, we report the development and use of the first genotoxicity biosensors employing phase II metabolic enzymes. We constructed NAT/DNA films designed to predict bioactivated genotoxicity of arylamines and investigated the influence of NAT-catalyzed metabolism of 2-AF on DNA damage. Results revealed that NAT mediated more rapid DNA damage from 2-AF in weakly acidic than at neutral pH.

EXPERIMENTAL SECTION

Chemicals and Materials. Arylamine acetyltransferase from pigeon liver (NAT, EC 2.3.1.5, 10% protein, 0.9 U/mg protein, pH 8.0, 25 °C, one unit acetylates 1.0 nmol *p*-nitroaniline/min, MW 33 000),⁴⁸ acetyl coenzyme A sodium salt (AcCoA), DL-dithiothreitol (DTT), ethylenediaminetetraacetic acid disodium salt dehydrate (EDTA), DNA (calf thymus, Type XV, 13 000 av base pairs, 41.9% G/C and salmon testes, 2000 av base pairs, 41.2% G/C), poly(guanylic acid) potassium salt (poly[G]), poly(cytidylic acid) potassium salt (poly[C]), poly(adenylic acid) potassium salt (poly[A]), tris(2,2'-bipyridyl)dichlororuthenium(II) hexahydrate, poly(diallyldimethylammonium chloride) (PDDA) and poly(sodium 4-styrenesulfonate) (PSS), 2-aminofluorene (2-AF), and *N*-acetyl-2-aminofluorene (2-AAF) were from Sigma-Aldrich. Water was purified with a Hydro Nanopure system to specific resistance > 16 M Ω . All other chemicals were reagent grade.

Voltammetry. Square wave voltammetry (SWV) was done using CH Instruments 660A and 430 electrochemical analyzers. The cell was protected from light and employed a saturated calomel reference electrode (SCE), Pt wire counter electrode, and a film-coated pyrolytic graphite (PG) disk as the sensor electrode. SWV conditions were 4 mV step height, 25 mV pulse height, and 5 Hz frequency with 95% ohmic drop compensated. The electrolyte solution was 10 mM acetate buffer, pH 5.5, containing 50 mM NaCl and 50 μ M Ru(bpy)₃²⁺ unless otherwise stated.

Sensor Construction. DNA–enzyme films were prepared by the layer-by-layer electrostatic assembly method⁴⁹ following an optimized protocol. Disks ($A = 0.15 \text{ cm}^2$) of ordinary basal plane PG (Advanced Ceramics) were abraded with 400 grit SiC paper

and sonicated in ethanol and pure water successively for 1 min, then rinsed with water and dried. Layers were formed by placing a drop of each adsorbate solution on the PG electrode for 15–20 min. NAT enzyme was adsorbed at 0 °C to maintain enzyme stability, and the electrode was then rinsed with water to remove weakly adsorbed enzyme and dried in a stream of nitrogen between adsorption steps. The times for steady state adsorption,⁴⁹ volume, and concentration of each adsorbate solution were (1) 15 min, 30 μ L of 2 mg mL⁻¹ PDDA in 50 mM NaCl; (2) 15 min, 30 μ L of 2 mg mL⁻¹ DNA in 5 mM pH 7.1 Tris buffer and 0.50 M NaCl; (3) 20 min, 20 μ L of 5 mg mL⁻¹ NAT in 50 mM pH 7.2 Tris buffer; and (4) 15 min, 30 μ L of 3 mg mL⁻¹ PSS 0.50 M NaCl. Final film architecture was denoted as the order of layer adsorption, i.e., PDDA/DNA/(NAT/DNA)₂ and (PDDA/DNA)₂. We refer to these as NAT/DNA and DNA films, respectively. Quartz crystal microbalance (QCM, USI Japan) was used to monitor film assembly at each step using gold coated QCM resonators (9 MHz, AT-cut, International Crystal Mfg. Co.). The gold-coated resonators were cleaned and derivatized before film deposition with 0.7 mM 3-mercapto-1-propanol and 0.3 mM 3-mercaptopropionic acid to mimic the negatively charged graphite surface as previously described.⁹

Enzyme Reactions in Films. Safety Note. 2-Aminofluorene and *N*-acetyl-2-aminofluorene are suspected human carcinogens. Procedures should be done in a closed hood while wearing gloves, using sealed cells. Stock solutions of 2-AF and 2-AAF were prepared in DMSO. Stock solutions of 20 mM DTT, EDTA, and AcCoA were prepared in water and kept at –20 °C. Incubations of DNA films were done in a thermostated vessel at 37 °C containing 2 mM 2-AF or 2-AAF in 10 mL of 10 mM pH 5.5 buffer. Incubations of NAT/DNA films for metabolite generation and reaction with DNA were done at 37 °C for the range of 0.5–5 min in 0.4 mL of 10 mM pH 5.8 buffer containing 1.5 mM 2-AF, 1 mM DTT, 1 mM EDTA, and 1.5 mM AcCoA in 1.5 mL microcentrifuge tube. The volume of DMSO was less than 10% of volume of incubation solution. After the reaction, the electrode was rinsed with water and transferred to an electrochemical cell containing Ru(bpy)₃²⁺ for SWV analysis.

NAT Activity Assay. For the solution assay, NAT (0.02–0.1 mg of protein) was dissolved in 1 mL of buffers (pH 4.5–7.5) containing 1 mM DTT, 1 mM EDTA, and 0.05 mM AcCoA. The reaction was initiated by addition of 10 μ L of 3 mM 2-AF in DMSO. After incubation at 37 °C for 30 min, the reaction mixture was eluted through a C18 Sep-Pak solid-phase extraction cartridge (Waters) for the isolation of the acetylated product (2-AAF) and unreacted 2-AF. 2-AAF and 2-AF were desorbed from the cartridge by eluting with 1 mL of methanol, and 20 μ L of the resulting solution was injected into a high-pressure liquid chromatograph (HPLC, Perkin-Elmer) with UV detection at 285 nm. An Ultra C18 (Restek) reversed-phase column (250 mm \times 4.6 mm, particle size 5 μ m) was used with 20 mM ammonium acetate (pH 4.5)/acetonitrile (50:50) at a flow rate of 1.0 mL min⁻¹. To assay immobilized NAT mediated N-acetylation of 2-AF, 10 electrodes of PDDA/(PSS/NAT)₃ were incubated in 5 mL of buffers (pH 7.2

(41) Levy, G. N.; Weber, W. W. *Carcinogenesis* **1989**, *10*, 705–709.

(42) Hung, C. F. *Neurochem. Res.* **2000**, *25*, 845–851.

(43) Chung, J. G.; Li, Y. C.; Lee, Y. M.; Lin, J. P.; Cheng, K. C.; Chang, W. C. *Leuk. Res.* **2003**, *27*, 831–840.

(44) Yang, C. C.; Chen, G. W.; Lu, H. F.; Wang, D. Y.; Chen, Y. S.; Chung, J. G. *Pharmacol. Toxicol.* **2003**, *92*, 287–294.

(45) Feng, Y.; Jiang, W.; Hein, D. *Toxicol. Appl. Pharm.* **1996**, *141*, 248–255.

(46) Josephy, P. D.; Evans, D. H.; Parikh, A.; Guengerich, F. P. *Chem. Res. Toxicol.* **1998**, *11*, 70–74.

(47) McQueen, C. A.; Chau, B. *Toxicol. Sci.* **2003**, *73*, 279–286.

(48) Andres, H. H.; Kolb, H. J.; Weiss, L. *Biochim. Biophys. Acta* **1983**, *746* (3), 182–92.

(49) (a) Lvov, Y. In *Protein Architecture: Interfacing Molecular Assemblies and Immobilization Biotechnology*; Lvov, Y., Möhwald, H., Eds.; Marcel Dekker: New York, 2000; pp 125–167. (b) Lvov, Y. In *Handbook of Surfaces And Interfaces Of Materials, Vol. 3. Nanostructured Materials, Micelles and Colloids*; Nalwa, R. W., Ed.; Academic Press: San Diego, CA, 2001, pp 170–189.

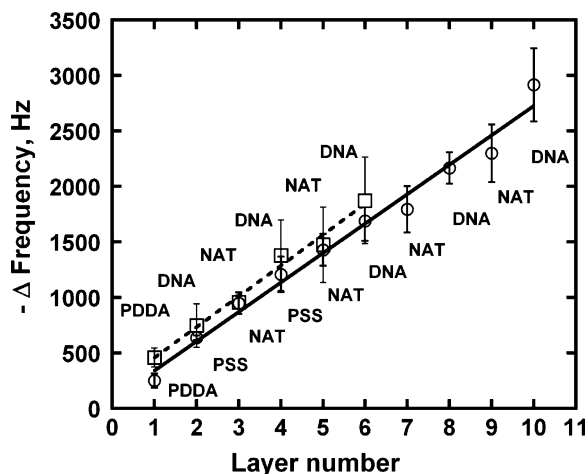


Figure 1. Quartz crystal microbalance frequency shifts for cycles of alternate adsorption on gold quartz resonators during preparation of PDPA/DNA/(NAT/DNA)₂ and PDPA/(PSS/NAT)₂/DNA/(NAT/DNA)₂ films.

and 5.8) containing 1 mM DTT, 1 mM EDTA, 0.1 mM AcCoA, and 0.03 mM 2-AF. After incubation at 37 °C for more than 4 h, the reaction mixture was analyzed by HPLC.

Capillary Liquid Chromatography–Mass Spectrometry (CapLC–MS/MS). For DNA adduct determinations, films of (PDPA/DNA)₂ were formed on hydroxylated 500 nm diameter fused-silica microspheres (Polysciences Inc., Warrington, PA). See Supporting Information for a full description of the procedures employed in the film formation and the reaction protocols. Briefly, the NAT/DNA films immobilized on the microspheres were exposed to 2 mM 2-AAF in 375 μL of pH 5.8 buffers/125 μL of acetonitrile for 24 h in stirred vessels at 37 °C, and then the reaction was stopped via centrifuging the microspheres from the solution. The centrifuged microspheres were resuspended in 0.5 mL of deionized water for neutral thermal hydrolysis,^{17a} followed by separation from the hydrolysate via centrifugation. The hydrolysate was filtered with a mass cutoff 3000 Da filter (Amicon, Beverly, MA) by injection into the CapLC–MS/MS. The capillary chromatograph (Waters capLC–XE) was equipped with a photodiode array (PDA) detector. The analytical column (Atlantis dC18, 150 mm × 0.3 mm, particle size 5 μm) and the trapping column (Atlantis dC18, 23.5 mm × 0.18 mm, particle size 5 μm) were from Waters (Milford, MA). One 10 μL injection of hydrolysate was loaded into the trapping column at a flow rate of 10.0 μL min⁻¹ and then flushed with water at a flow rate of 10.0 μL min⁻¹. Trapped adducts were then back-flushed from the trapping column onto the analytical column at a flow rate of 4.25 μL min⁻¹ with the gradient of 50% B for 10 min, 50–75% B for 10–15 min, 75% B for 15–35 min (A: 10 mM acetate buffer pH 5.5, B: methanol). Electrospray ionization-mass spectrometry (ESI-MS) employed a Micromass Quattro II (Beverly, MA) operated in the positive ion mode. Identification of adduct peaks was done using multiple reaction monitoring (MRM) at a cone voltage of 15 V, collision energy of 15 eV, and collision gas (Ar) pressure of 5 × 10⁻³ mbar.

RESULTS

Sensor Film Characterization. Figure 1 shows the average change in QCM frequency ($-\Delta F$), proportional to mass/area (μg cm⁻²),⁴⁹ upon sequential adsorption of individual PDPA, DNA,

and NAT layers on a gold-quartz QCM resonator to make PDPA/DNA/(NAT/DNA)₂ and PDPA/(PSS/NAT)₂/DNA/(NAT/DNA)₂ films. The isoelectric point of NAT is 4.8,⁴⁸ and adsorbate solution pHs of 7.2 and 5.8 gave the same adsorbed mass of NAT in the films. Thus, NAT was adsorbed onto the sensor surface from a neutral pH buffer. As Figure 1 and Table 1 show, NAT adsorbed in sufficient quantities under these conditions even though NAT is slightly negative. Adsorption on the negative DNA layers is most likely related to localized charge on the enzyme surface, as documented for other enzymes.⁵⁰ The presence of NAT on the electrode was confirmed by LC measurement of NAT activity (see below). Overall, reproducible increases in $-\Delta F$ versus layer number (Figure 1) indicated reproducible and stable film growth. Table 1 summarizes the surface coverage of DNA and NAT and nominal film thickness obtained from QCM. The total amount of DNA averaged 0.7 pmol cm⁻² and NAT was 52 pmol cm⁻² for PDPA/DNA/(NAT/DNA)₂ and 130 pmol cm⁻² for PDPA/(PSS/NAT)₂/DNA/(NAT/DNA)₂ films.

Direct DNA Damage from 2-AAF. In exploratory studies, DNA films without NAT were exposed to 2-AAF, the metabolite of 2-AF, to evaluate DNA damage. SWV peaks for oxidation of the guanines in DNA catalyzed by Ru(bpy)₃²⁺ were found at +1.05 V vs SCE (Figure 2a) as expected.^{9,13} The catalytic pathway (Scheme 3) is similar to that reported for DNA in solution.¹³ Figure 2a shows that the oxidation peaks increased and became broader after DNA films reacted with 2-AAF at pH 5.5. As documented for sensors using DNA and cyt P450s,^{9,11,12,18} the peak current increase is caused by an increased catalytic reaction rate resulting from chemical damage of DNA and better access of the catalyst to guanines in the partial disrupted DNA double helix.

Figure 2b shows the control SWV response after exposure of DNA films to 2-AF. The oxidation peak remained unchanged after incubation, showing that 2-AF does not react with DNA under these conditions. However, an additional peak appeared at 0.43 V vs SCE. We observed similar peaks at 0.43 V vs SCE when bare PG or single stranded polynucleotide (PDPA/X)₂ films (X = poly G, poly A, or PSS) were incubated with 2-AF. (Supporting Information, Figure S1). These results show that the new peak at 0.43 V is due to the direct oxidation of 2-AF.

The ratio of SWV peak currents at specific incubation times to that with no incubation (Figure 3) increased with 2-AAF exposure up to 5 min, then increased more slowly at longer times. The rate of signal increase is faster at pH 5.5 than at pH 7.2. This suggests that DNA damage from 2-AAF occurs more readily in slightly acidic solutions. Control sensors exposed to 2-AF gave no signal increase.

To assess the cause of broadening of the oxidation peak after incubation with 2-AAF (Figure 2a), films containing single stranded polynucleotides were reacted with 2-AAF. Oxidation peaks with poly A and poly C films were found at around 0.90 V vs SCE (Figure 4), slightly negative of the catalytic peak. Poly A and poly C do not react with Ru(bpy)₃³⁺,¹³ so this 0.9 V peak can be attributed to direct oxidation of 2-AAF. For poly G, which does react with the catalyst, a broader catalytic peak was found similar to the DNA films, with a significant increase in peak current. The difference of the 3 and 0 min peaks in Figure 4 gave a double

(50) Schenkman, J. B.; Jansson, I.; Lvov, Y. M.; Rusling, J. F.; Boussaad, S.; Tao, N. J. *Arch. Biochem. Biophys.* **2001**, *385*, 78–87.

Table 1. Average Characteristics of NAT/DNA Films from QCM Results

film	thickness ^a (nm)	total mass DNA ^b ($\mu\text{g cm}^{-2}$)	total mass NAT ($\mu\text{g cm}^{-2}$)
PDDA/DNA/(NAT/DNA) ₂	30 ± 4	6.1 ± 0.3	1.7 ± 0.3
PDDA/(PSS/NAT) ₂ /DNA/(NAT/DNA) ₂	47 ± 3	6.2 ± 0.3	4.3 ± 0.5

^a From $d = (-0.016 \pm 0.002)\Delta F$ (in nm). ^b From M/A (g cm^{-2}) = $-\Delta F$ (in Hz)/(1.83 × 10⁸); see ref 49 for details.

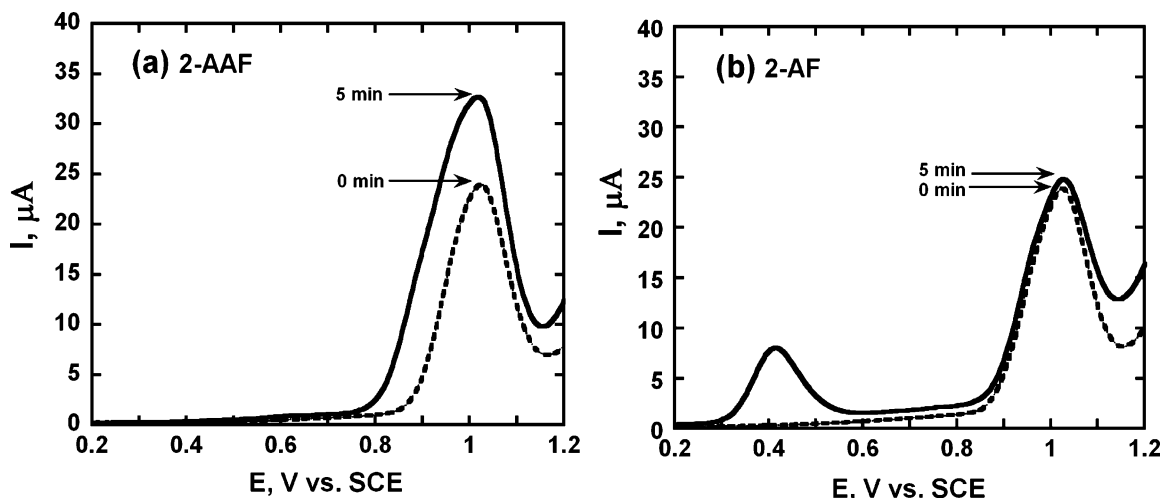


Figure 2. SWVs of (PDDA/DNA)₂ films on PG electrodes in pH 5.5 buffer containing 50 μM $\text{Ru}(\text{bpy})_3^{2+}$ before (0 min) and after (5 min) incubations at 37 °C with (a) 2 mM 2-acetylaminofluorene and (b) 2 mM 2-aminofluorene.

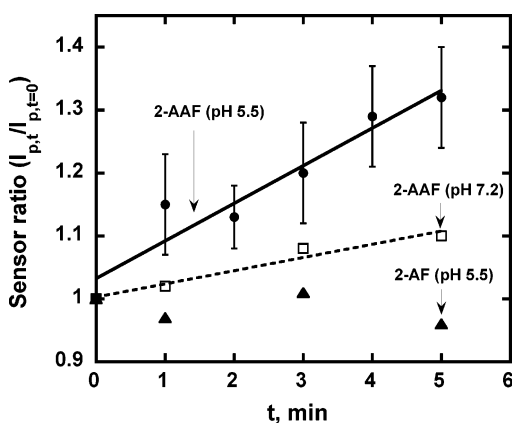
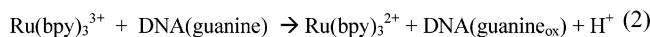
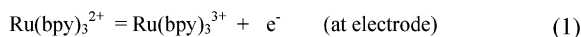


Figure 3. Influence of incubation time and pH on the catalytic peak currents for (PDDA/DNA)₂ films reacted at 37 °C with 2-acetylaminofluorene in two incubation buffers, pH 5.5 (●) and pH 7.2 (□), and 2-aminofluorene (▲) (av error from $n = 3-8$ trials was ~8%).

Scheme 3



peak and showed that the broad peak after the 2-AAF incubation was attributable to overlapped peaks for direct oxidation of 2-AAF at 0.9 V vs SCE superimposed on the catalytic oxidation peak for poly G at 1.05 V.

Characterization of Enzyme Activity. Figure 5a is a liquid chromatogram (LC) showing the conversion of 2-AF to 2-AAF by AcCoA-dependent NAT enzyme in solution along with controls without NAT. Figure 5b shows the same comparison where 2-AAF was formed from NAT immobilized on PG electrodes as PDDA/

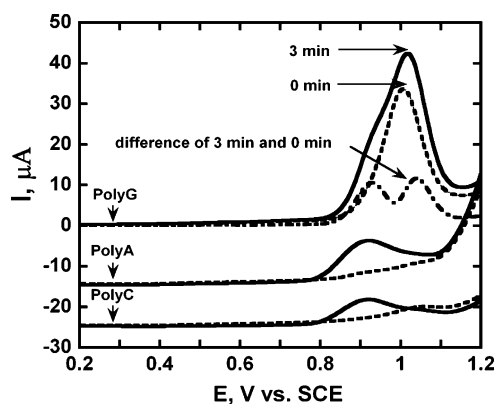


Figure 4. SWVs of (PDDA/poly G)₂, (PDDA/poly A)₂, and (PDDA/poly C)₂ films in pH 5.5 acetate buffer containing 50 μM $\text{Ru}(\text{bpy})_3^{2+}$ before (0 min, dashed line) and after (3 min, solid line) incubations at 37 °C with 2 mM 2-AAF in pH 5.5 buffer.

(PSS/NAT)₃ along with controls without enzyme films. These data clearly show that 2-AAF was formed when NAT was present. Further analysis of the 2-AF conversion by immobilized NAT was done using CapLC-MS. Similar NAT films formed on silica microspheres were exposed to identical conditions as electrode bound NAT and the identity of 2-AAF in the reaction medium was confirmed from mass spectral analysis (Supporting Information, Figure S2).

To establish optimal pH for NAT activity and NAT-mediated DNA damage, N-acetylation of 2-AF was determined by LC over a range of pH values. Figure 6 shows that pH 7.5 offered the best NAT activity consistent with an earlier report.⁵¹ However, Figure 3 shows that DNA damage from direct 2-AAF exposure occurred

(51) Chang, F. C.; Chung, J. G. *Curr. Microbiol.* **1998**, *36*, 125–130.

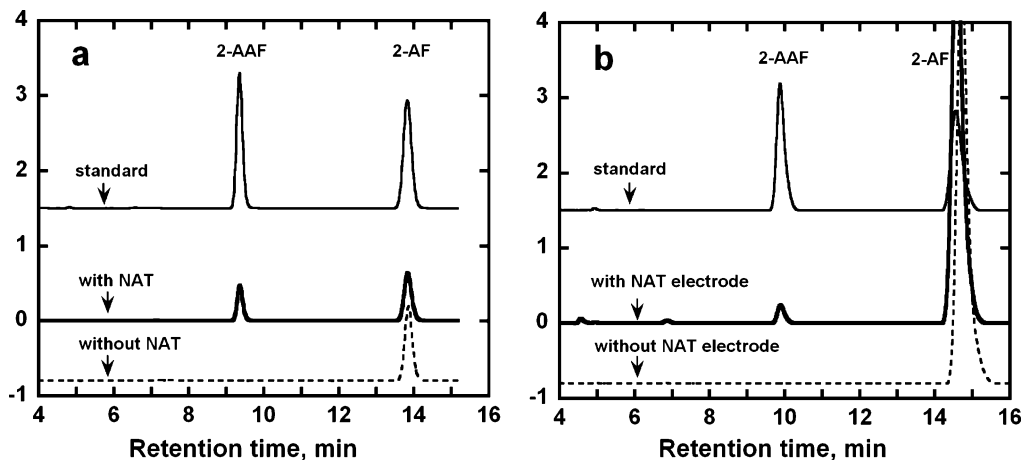


Figure 5. Liquid chromatograms of (a) dissolved NAT ($25 \mu\text{g mL}^{-1}$) incubated in 1 mL of pH 7.2 buffer containing 0.03 mM 2-AF, 0.05 mM AcCoA, 1 mM DTT, and 1 mM EDTA at 37°C for 30 min, (b) PDDA/(PSS/NAT) $_3$ (133 pmol cm^{-2}) on 10 PG electrodes incubated in 5 mL of pH 7.2 buffer containing 0.03 mM 2-AF, 0.1 mM AcCoA, 1 mM DTT, and 1 mM EDTA at 37°C for 4 h.

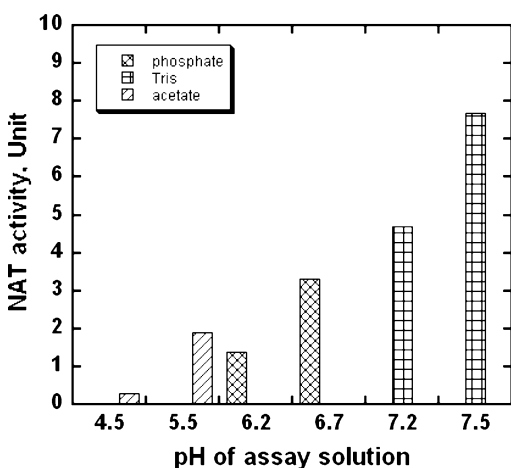


Figure 6. Influence of pH on relative NAT activity in the presence of NAT ($25 \mu\text{g mL}^{-1}$), 0.03 mM 2-AF, 0.05 mM AcCoA, 1 mM DTT, and 1 mM EDTA at 37°C for 30 min. (Unit: one unit will acetylate 1.0 nmol of 2-AF per min per mg protein at 37°C .)

most rapidly under slightly acidic conditions. NAT retains $\sim 25\%$ of its activity at pH 5.5–5.8 relative to pH 7.5 (Figure 6). Related studies showed that the relative activity of NAT immobilized on PG electrodes and microspheres using pH 5.8 buffer was comparable with the solution results (data not shown). Despite lower activity, pH 5.8 was found to provide sufficient 2-AF conversion for the sensors and was used for subsequent experiments.

Metabolite-Generated DNA Damage. We incorporated NAT into films on PG electrodes to make sensors that monitor DNA damage arising from bioactivation of 2-AF. These sensors were exposed to solutions of 2-AF and AcCoA in the pH 5.8 reaction medium.

Figure 7 shows typical SWV responses before (0 min) and after exposure (5 min) to the 2-AF/AcCoA reaction medium. The increase in peak current at approximately 1.0 V vs SCE is evident and suggests that DNA damage has occurred. This is consistent with the activation of 2-AF by NAT to form reactive 2-AAF in the films. 2-AF is not capable of binding directly to DNA, as described above. At pH 7.2, much smaller SWV peak current increases were seen for NAT/DNA films exposed to 2-AF/AcCoA, consistent with the slower reaction of 2-AAF with DNA at this pH (cf. Figure 3).

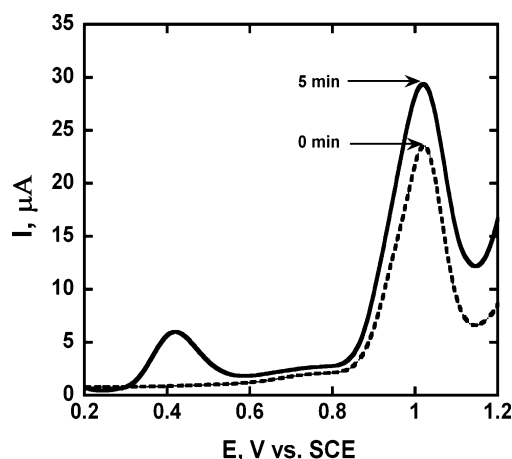


Figure 7. SWVs of PDDA/DNA/(NAT/DNA) $_2$ sensor films in pH 5.8 buffer containing $50 \mu\text{M Ru}(\text{bpy})_3^{2+}$ before (0 min) and after (5 min) incubations at 37°C in pH 5.8 incubation solution containing 1.5 mM 2-AF, 1.5 mM AcCoA, 1 mM DTT, and 1 mM EDTA.

Figure 8 shows peak ratios for NAT/DNA films with increasing exposure to the 2-AF/AcCoA medium that increased over 2–3 min followed by a leveling off at longer times. This ratio plot suggests that DNA damage increased in a similar fashion to the direct damage experiments (cf. Figure 3). Controls without AcCoA or NAT gave no signal increase.

The sensor ratio for PDDA/DNA/(NAT/DNA) $_2$ with 52 pmol cm^{-2} NAT reached a maximum of 1.27, significantly above the controls (~ 1) but is not as large as for cyt P450 enzymes in similar sensors.⁹ An increase in signal was obtained by increasing NAT concentration in the films by including four NAT layers, using PDDA/(PSS/NAT) $_2$ /DNA/(NAT/DNA) $_2$ to obtain 130 pmol cm^{-2} NAT. (QCM analysis is shown in Figure 1.) Figure 8 shows that doubling the amount of NAT in the films increased the damage ratio by $\sim 20\%$ over 5 min.

Relative enzyme turnover rates can be estimated using these sensors with DNA damage as the analytical endpoint.^{1,8} The initial slope of the sensor ratio plots (Figure 8) depend on the rate of NAT-catalyzed formation of 2-AAF and its rate of reaction with DNA. On the basis of the amount of enzyme in the films estimated from QCM (Table 1) and the initial slope of the sensor ratio plots (Figure 8), the relative NAT turnover rate at pH 5.8 for production

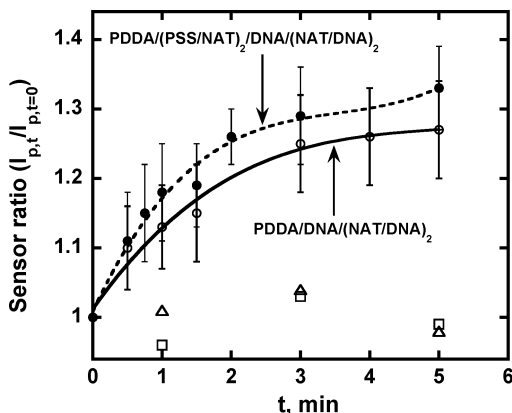


Figure 8. Influence of incubation time in pH 5.8 buffer containing 1.5 mM 2-AF, 1.5 mM AcCoA, 1 mM DTT, 1 mM EDTA for two architectures of PDDA/DNA/(NAT/DNA)₂ (52 pmol cm⁻² NAT) and PDDA/(PSS/NAT)₂/DNA/(NAT/DNA)₂ (130 pmol cm⁻² NAT) on peak currents. Control 1 (□), no AcCoA in buffer; control 2 (△), no NAT using the (PDDA/DNA)₂ film (av error in controls from 3 to 8 trials was ±8%).

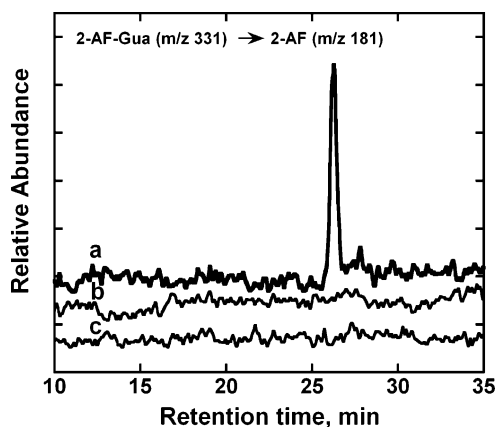


Figure 9. MRM ion chromatograms measuring the m/z 331 \rightarrow 181 transition for neutral hydrolysates of reaction mixtures obtained after 24 h incubations using films on 500 nm silica microspheres (a) (PDDA/DNA)₂ film incubated in 2 mM 2-AAF. (b) Control 1, PDDA film (no DNA) incubated in 2 mM 2-AAF. (c) Control 2, (PDDA/DNA)₂ film incubated without 2-AAF. All reactions were in pH 5.5 buffer.

of 2-AAF was 13 (nmol NAT)⁻¹ min⁻¹ for PDDA/DNA/(NAT/DNA)₂ and 9 (nmol NAT)⁻¹ min⁻¹ for PDDA/(PSS/NAT)₂/DNA/(NAT/DNA)₂ films. The lower relative turnover for the PSS/NAT precursor layering scheme despite a higher overall signal may reflect decreased catalytic accessibility of DNA layers positioned further from the electrode surface.

LC-MS Analysis of DNA Adduct. Nucleobase adduct formation from the reaction of 2-AAF with DNA in films was confirmed by CapLC-MS/MS. To obtain a sample with sufficient DNA adducts, reactions of 2-AAF were run with DNA films constructed on 500 nm silica microspheres for 24 h. These films were exposed to 2-AAF in buffer, then neutral thermal hydrolysis of the films was done to obtain samples enriched in guanine adducts.^{17a} Figure 9 shows the multiple reaction monitoring (MRM) transition m/z 331 \rightarrow 181 corresponding to MH⁺ of 2-AAF-guanine fragmenting to protonated 2-AAF. The presence of this species in the reaction medium is consistent with previous reports of the same pattern of adduct fragmentation when 2-AAF adducted guanines from DNA

were analyzed by MRM⁵² and strongly suggests formation of guanine adducts in our sensor films. No peak with this m/z transition was found in the controls.

DISCUSSION

Phase I enzymes account for approximately 75% of drug metabolism, with cyt P450 enzymes responsible for the majority of that figure.⁵³ However, of metabolites unaccounted for by cyt P450s, phase II enzymes play important roles and may be critical for certain molecular types.^{19,21} The results above demonstrate that a phase II enzyme, NAT, can be incorporated into an electrochemical genotoxicity sensor platform¹⁰ for rapid measurement of relative genotoxicity arising from reactive metabolites resulting from that enzyme alone.

DNA damage by NAT metabolites of 2-AF is suggested by the increase in sensor peak ratio (Figure 8). Peak increases for similar sensors incubated with other metabolites has been correlated with increased amounts of major nucleobase adducts with time as measured by LC-MS.^{17,18} In the present work, assignment of the sensor response to DNA damage in the sensor films is strongly supported by lack of response for controls (Figure 8), by the chromatographic detection of 2-AAF from NAT conversion of 2-AF in films (Figure 5b), and by LC-MS detection of 2-AAF-guanine adducts in DNA films after reaction with 2-AAF (Figure 9).

Sensor response vs reaction time relates to relative enzyme turnover (Figure 8). As reported in the results section, sensor-derived turnover rates were 9–13 (nmol NAT)⁻¹ min⁻¹ depending on film configuration. NAT metabolizes 2-AF *in vivo*,²⁹ and its turnover in the sensors suggests that the film environment does not compromise activity to any great extent. TD_{LO} is an *in vivo* toxicity metric defined as the lowest dose that produces tumorigenic effects. In mice exposed to 2-AF, TD_{LO} was 100 mg kg⁻¹ for oral and 50–100 mg kg⁻¹ for implanted administration,^{54a,b} suggesting that the sensor derived responses can be linked to genotoxic effects. Additional sensor work using standard conditions for a broad range of chemicals is planned to explore such relationships further.

The carcinogenesis of arylamines has been well studied, most notably by the pioneering work of Miller and Miller.^{55–58} Pathways of 2-AF metabolism *in vivo* follow two main routes, summarized in Scheme 4.^{37,39,55} In one pathway, 2-AF (**1**) undergoes initial N-oxidation, primarily by cyt P450 1A2 in humans, resulting in a hydroxylated aminofluorene, N-OH-2-AF (**4**).¹⁹ Alternative phase II metabolism via sulfotransferase or O-acetyltransferase yields ultimate carcinogens due to the excellent leaving group imparted by the ester. Upon ester removal, the resulting reactive metabolite is a nitrenium ion (**5**) and this electrophilic moiety attacks guanine at the C8 position resulting in a 2-AAF-guanine adduct (**7**). Alternatively, **4** has been shown to bind directly to DNA without undergoing further metabolism, presumably through acid-catalyzed hydrolysis, which is discussed in more detail below. In the second pathway, 2-AF is converted to 2-AAF (**2**) by cytosolic

(52) Wolf, S. M.; Vouros, P. *Chem. Res. Toxicol.* **1994**, *7*, 82–88.

(53) Guengerich, F. P. *AAPS J.* **2006**, *8*, E101–E111.

(54) (a) Wilson, R. H.; DeEds, F.; Cox, J. A. *Cancer Res.* **1947**, *7*, 453–458. (b) Clayson, D. B.; Jull, J. W.; Bonser, G. M. *Brit. J. Cancer* **1958**, *12*, 222–230.

(55) Miller, E. C. *Cancer Res.* **1978**, *38*, 1479–1496.

(56) Miller, E. C.; Miller, J. A.; Enomoto, M. *Cancer Res.* **1964**, *24*, 2018–2031.

(57) Kadlubar, F. F.; Miller, J. A.; Miller, E. C. *Cancer Res.* **1977**, *37*, 805–814.

(58) Josephy, P. D.; Gruz, P.; Nohmi, T. *Mutat. Res.* **1997**, *386*, 1–23.

does not undergo extensive oxidative metabolism by cyt P450s.^{37,55,56} However, upon administration to liver, mammary gland, and bladder in mice and hamsters, 2-AAF was as carcinogenic as 2-OH-AAF.⁵⁶ These results suggest that hydroxylation of 2-AAF by cyt P450 is involved in producing tumors in rodents.⁵⁶

In the present work, we found that direct exposure to 2-AAF or 2-AAF generated via NAT biocatalysis *in vitro* produced DNA damage. In addition to the sensor results (Figures 3, 7, and 8), LC-MS (Figure 9) confirmed that 2-AF-guanine adducts formed from exposure of immobilized DNA to 2-AAF under weakly acidic conditions. The m/z 331 \rightarrow 181 in the chromatogram (Figure 9) corresponds to the 2-AF-guanine adduct fragmenting to 2-AF. The absolute location of 2-AF on guanine cannot be determined since both C8 and N² adducts have m/z 331. However, these results are consistent with the reaction pathway in Scheme 4. In this pathway, a reactive nitrenium intermediate **5** formed after acid catalyzed amide hydrolysis^{60–62} of 2-AAF **2** may attach guanine at C8 or rearrange to carbonium ion **6** and attach at guanine N².

DNA damage by 2-AAF detected by our sensors is facilitated by the film reaction environment. The sensor film provides high concentrations of DNA intermixed with enzyme,⁴⁹ so that 2-AAF is formed in a tiny reaction volume with a high concentration of reactive DNA sites. On the basis of QCM analysis (Table 1), $\sim 6 \mu\text{g cm}^{-2}$ DNA is present in the film, of which 45% is G-C (0.6 nmol). MS results (Figure 9) and the preferential reaction of 2-AAF with poly G in the sensors (Figure 4) are consistent with prior reports showing guanine as the primary adduct site for reactions with arylamines.^{40,63}

Figure 2 suggests that slightly acidic conditions provide greater DNA damage from exposure to 2-AAF than neutral buffers. We

previously found that epoxides and methylating agents were more reactive toward DNA at acidic pH.⁶⁴ Kadlubar et al. found that arylamine metabolites were 10–25 times more reactive toward DNA at lower pH.⁵⁷ As discussed above, several reports suggested that phase II conjugations or phase I oxidations are necessary to impart genotoxicity to 2-AAF. In contrast, our studies here did not employ a secondary enzyme. Under these experimental conditions, 2-AAF is still shown to have DNA-damaging properties, which may have *in vivo* relevance. DNA adducts in bladder cells were shown to be due to the hydrolysis to hydroxylated arylamines that occur in the acidic urine. Furthermore, N-acetyltransferase polymorphism plays a significant role in 2-AF-DNA adduct formation in the urinary bladder.^{33,45} In our *in vitro* sensors, we employed similar acidic conditions and show that 2-AAF alone can damage DNA. It is conceivable that some DNA adducts formed *in vivo* could be due to NAT metabolism of 2-AF at mildly acidic pH. This finding may shed new light on the etiology of these molecules in the formation of bladder cancers.

In summary, results herein show for the first time that phase II enzymes can be used in electrochemical sensors to detect genotoxicity via a DNA-damage endpoint. Reaction conditions imparted by sensor films and mildly acidic pH revealed DNA damage by 2-AAF. Future efforts will focus on the combination of phase I and II metabolism in arrays, in addition to pinpointing the exact mechanism of DNA damage from 2-AAF in these films.

ACKNOWLEDGMENT

This work was supported by the National Institute of Environmental Health Services (NIEHS) of the NIH via US PHS Grant No. ES03154.

SUPPORTING INFORMATION AVAILABLE

Additional information as noted in text. This material is available free of charge via the Internet at <http://pubs.acs.org>.

Received for review August 22, 2007. Accepted November 7, 2007.

AC701781Y

(61) Antonczak, S.; Ruiz-Lopez, M. F.; Rivail, J. L. *J. Am. Chem. Soc.* **1994**, *116*, 3912–3921.

(62) Brown, R. S.; Bennet, A. J.; Slebocka-Tilk, H. *Acc. Chem. Res.* **1992**, *25*, 481–488.

(63) Zhou, L.; Rajabzadeh, M.; Traficante, D. D.; Cho, B. P. *J. Am. Chem. Soc.* **1997**, *119* (23), 5384–5389.

(64) Munge, B.; Estavillo, C.; Schenkman, J. B.; Rusling, J. F. *Chem. Bio. Chem.* **2003**, *4*, 82–89.